DOI: 10.1111/exd.12144
www.blackwellpublishing.com/EXD

Letter to the Editor

Nanoscale infrared (IR) spectroscopy and imaging of structural lipids in human stratum corneum using an atomic force microscope to directly detect absorbed light from a tunable IR laser source

Curtis Marcott[1], Michael Lo[2], Kevin Kjoller[2], Yegor Domanov[3], Guive Balooch[4] and Gustavo S. Luengo[3]

[1]Light Light Solutions, LLC, Athens, GA, USA; [2]Anasys Instruments Inc., Santa Barbara, CA, USA; [3]L'Oréal Research and Innovation, Aulnay sous Bois, France; [4]L'Oréal Research and Innovation, Clark, NJ, USA

Correspondence: Curtis Marcott, Light Light Solutions, LLC, PO Box 81486, Athens, GA 30608-1486, USA, Tel.: +1-513-720-0171, e-mail: marcott@lightlightsolutions.com; Gustavo S. Luengo, L'Oréal Research and Innovation, Aulnay sous Bois, France, Tel.: +33 158317173, e-mail: gluengo@rd.loreal.com

Abstract: An atomic force microscope (AFM) and a tunable infrared (IR) laser source have been combined in a single instrument (AFM-IR) capable of producing ~200-nm spatial resolution IR spectra and absorption images. This new capability enables IR spectroscopic characterization of human stratum corneum at unprecendented levels. Samples of normal and delipidized stratum corneum were embedded, cross-sectioned and mounted on ZnSe prisms. A pulsed tunable IR laser source produces thermomechanical expansion upon absorption, which is detected through excitation of contact resonance modes in the AFM cantilever. In addition to reducing the total lipid content, the delipidization process damages the stratum corneum morphological structure. The delipidized stratum corneum shows substantially less long-chain CH_2-stretching IR absorption band intensity than normal skin. AFM-IR images that compare absorbances at 2930/cm (lipid) and 3290/cm (keratin) suggest that regions of higher lipid concentration are located at the perimeter of corneocytes in the normal stratum corneum.

Key words: atomic force microscopy – infrared microspectroscopy – infrared – skin – stratum corneum

Accepted for publication 1 April 2013

Background

The stratum corneum (SC), the outermost layer of the epidermis of human skin, fulfils the important functions of helping to regulate water loss and acting as a barrier to foreign substances. It consists of corneocytes surrounded by an intercellular lipid matrix, sometimes referred to as a 'bricks and mortar' structure (1–3). The SC is typically about 10–25 cell layers thick (~5–50 μm). Corneocytes are cells without nuclei filled with keratin filaments, amino acids and other small molecules collectively referred to as natural moisturizing factor (NMF), which are derived from the breakdown of filaggrin, a protein that surrounds keratin filaments. A highly cross-linked protein shell surrounds the corneocyte, which together with the keratin filaments accounts for both the flexibility and mechanical resilience of the SC. The SC contains about 20% water, part of which is tightly bound to hygroscopic molecules (the NMF) and lipids in the skin. This fraction of water content is proportional to external relative humidity. The remaining not free water is bound within the intracellular keratin and usually does not change much in healthy humans.

It is believed that many ingredients in topically applied drugs act through penetrating the SC barrier layer via a winding route through the thin lipid matrix phase ('mortar') that surrounds corneocytes ('bricks'). Thus, the ability to visualize the distribution of lipidic components of the SC is important for gaining a better understanding of how chemical substances penetrate through the skin. For additional background, see Data S1, Supporting Information (4–17).

Questions addressed

The main aim of this study is to demonstrate how the new methodology of AFM-IR spectroscopy and imaging can be used to provide unprecedented insights, although higher spatial resolution and chemical specificity, into the location of lipid components in stratum corneum cross-sections.

Experimental design

For experimental design, see Data S1, Supporting Information (18).

Results

Figure 1 shows AFM topography images (a, c) and IR spectra (b, d) collected from the locations indicated on the image for the delipidized SC sample (a, b) and the normal SC sample that has not been delipidized (c, d). The colour of the spectrum corresponds to the colour of the marker location on the AFM image, and the number label on the marker location represents the ratio of the 2856/cm baseline-corrected integrated band intensity divided by the 3290/cm baseline-corrected integrated band area. The boxes drawn on the spectra outline the spectral regions used for determining the band areas, and the dark blue lines represent the approximate baseline used.

As seen with other treatments (19), the delipidization procedure is observed to degrade the morphological structure of the SC. The normal SC sample also exhibits evidence of substantially more long-chain CH_2 groups due to the lipid component in all the 18 IR spectra shown. It also appears from these spectra that the lipid component is evenly distributed within the limited selection of spectra. When a single spectrum representing the average of all 18 spectra for the normal SC sample shown in Fig. 1b is

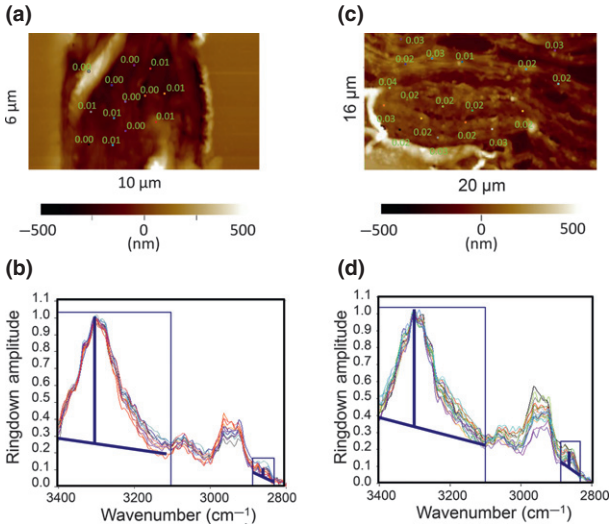

Figure 1. Contact-mode AFM height image (a) and 13 AFM-IR spectra (b) of a delipidized SC cross-section. Contact-mode AFM height image (c) and 18 AFM-IR spectra (d) of a normal SC cross-section. The coloured marker locations (each representing a 20 × 100 nm area of the sample) on the AFM images (a, c) are labelled with the ratio of the baseline-corrected band intensities of the 2856 and 3290/cm peaks corresponding to the spectrum of the same colour.

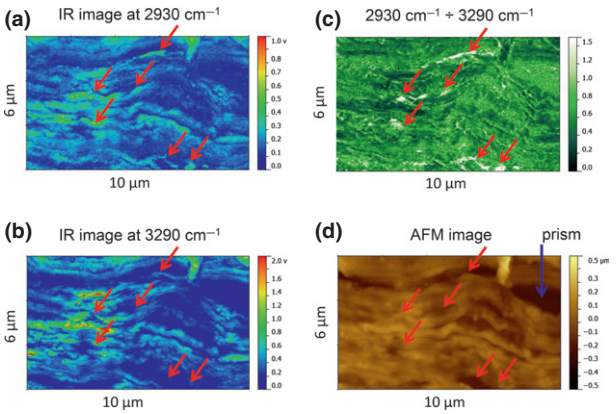

Figure 2. AFM-detected IR images collected from the same area near the upper left corner of the normal SC sample shown in Fig. 1c. (a) IR absorbance image collected with the laser source tuned to the fixed wavenumber of 2932/cm; (b) IR absorbance image collected with the laser source tuned to the fixed wavenumber of 3290/cm; (c) ratio of IR images shown in (a) and (b) (2932/cm per 3290/cm); (d) AFM topography image. Red arrows indicate locations of high lipid concentration. The blue arrow on the AFM image (d) indicates a region where the bare ZnSe prism is exposed.

compared with a corresponding plot showing the average of the 13 IR spectra shown in Fig. 1d, it becomes clear there is much less lipid component in the delipidized SC sample, as evidenced by a much weaker absorbance signal at 2856/cm due to the long-chain CH_2 symmetric stretching band (data not shown, see Figure S1, Supporting Information).

Figure 2 shows four separate AFM-detected images of the same area of the normal SC sample including the upper left corner of Fig. 1c. Figure 2a,b shows individual IR images collected using AFM detection with the pulsed IR laser source held at the fixed wavenumbers of 2930 and 3290/cm, respectively. An image representing the ratio of absorbances at 2930 and 3290/cm is shown in Fig. 2c, and the corresponding AFM topography image is shown in Fig. 2d. Although the keratin/protein and NMF components in the corneocytes do show significant IR absorbance in the aliphatic CH_2-stretching region between 3000 and 2800/cm, the IR absorbance at 2930/cm becomes much stronger when lipids are present. This is because an IR absorption band due to the CH_2 antisymmetric stretching vibrational modes in long hydrocarbon chains occurs near 2930/cm. Thus, IR absorption intensity at this wavelength will be stronger where there is a higher lipid content. The broad IR band centred at 3290/cm is mostly due to the amide A (NH-stretching) vibration from the keratin/protein component of SC, although OH-stretching vibrations also absorb in this region. The red arrows on each of the four images point to locations with high lipid content. These locations are all found at the perimeter of the corneocytes. Interestingly, the lipid component in the 'mortar' region between the corneocytes does not appear to be continuous in the normal SC sample, but rather exists in specific pockets of higher concentration. This may be the result of sample preparation, embedding, and sectioning processing producing air gaps and a pooling of lipids around the perimeter of the corneocytes. The detailed distribution of the lipid content reported here goes well beyond what has been previously obtained using other spectroscopy techniques.

Conclusions

A new approach using AFM to detect light absorption from a pulsed tunable IR laser source enables spectroscopic characterization of the human stratum corneum to be spectroscopically characterized at unprecedented levels. Studies of thin cross-sections of the normal and delipidized stratum corneum indicate that in addition to reducing the total lipid content, the delipidization process damages the stratum corneum structure as measured by AFM. The delipidized stratum corneum shows substantially less long-chain CH_2-stretching IR absorption band intensity than normal stratum corneum. AFM-IR images, which compare absorbances at 2930/cm (lipid) and 3290/cm (keratin), suggest that regions of higher lipid concentration are located at the perimeter of the corneocytes in normal stratum corneum. This work suggests that future AFM-IR studies may prove useful for understanding penetration pathways through the stratum corneum of specific ingredients in topically applied drugs or skin care products.

Acknowledgements

We thank NIST-ATP Award #70NANB7H7025 and the National Science Foundation award NSF-SBIR 0750512 for providing the financial support. We are grateful to Anne-Marie Minondo for preparing thin sections of the stratum corneum.

Author contributions

GSL designed the research study; GSL, YD and ML performed the research; ML and CM analysed the data; CM wrote the manuscript; ML, KK, GSL and GB edited the manuscript.

Conflict of interests

The authors state no conflict of interest.

References

1 Rawlings A V, Harding C R. Dermatol Therapy 2004: **17**: 43–48.

2 Verdier-Sevrain S, Bonte F J. Cosmetic Dermatol 2007: **6**: 75–82.

3 Hoath S B, Leahy D J. Formation and function of the stratum corneum. In: Marks R, Lévêque J L,

Voegeli R, eds. The Essential Stratum Corneum. London: Martin Dunitz, 2002: 741–746.
4 Rawlings A V, Scott I R, Harding C R *et al.* J Invest Dermatol 1994: **103**: 731–741.
5 Potts R O, Guzek D B, Harris R R *et al.* Arch Dermatol Res 1985: **277**: 489–495.
6 Lucassen G W, Van Veen G N A, Jansen J A J. J Biomed Opt 1998: **3**: 267–280.
7 Caspers P J, Lucassen G W, Carter E A *et al.* J Invest Dermatol 2001: **116**: 434–442.
8 Crowther J, Sieg A, Blenkiron P *et al.* Brit J Dermatol 2008: **159**: 567–577.
9 Wollny G, Brundermann E, Arsov Z *et al.* Opt Express 2008: **16**: 7453–7459.
10 Busch K, Konig M, Niegemann J. Laser Photonics Rev: 2011: 1–37.
11 Kazarian S G, Chan K L A. Appl Spectrosc 2010: **64**: 135A–152A.
12 Gulley-Stahl H J, Bledsoe S B, Evan A P *et al.* Appl Spectrosc 2010: **64**: 15–22.
13 Nasse M J, Walsh M J, Mattson E C *et al.* Nat Methods 2011: **8**: 413–416.
14 Dazzi A, Glotin F, Carminati R. J Appl Phys 2010: **107**: 124519.
15 Dazzi A, Prazeres R, Glotin F *et al.* Ultramicroscopy 2008: **108**: 635–641.
16 Prater C, Kjoller K, Cook D *et al.* Microsc Anal 2008: **24**: 5–8.
17 Marcott C, Lo M, Kjoller K *et al.* Appl Spectrosc 2011: **65**: 1145–1150.
18 Garson J C, Doucet J, Leveque J L *et al.* J Invest Dermatol 1991: **96**: 43–49.
19 Quan T, Qin Z, Shao Y *et al.* J Exp Dermatol 2011: **20**: 572–576.

Supporting Information

Additional Supporting Information may be found in the online version of this article:

Figure S1. Average of the 13 dilipidated SC AFM-IR spectra shown in Fig. 1b (top).

Data S1. Additional background and experimental design sections.